remote sensing

MDPI

Article

Hydrological Response of Alpine Wetlands to Climate Warming in the Eastern Tibetan Plateau

Wenjiang Zhang [1], Yonghong Yi [2], Kechao Song [1,*], John S. Kimball [2] and Qifeng Lu [3]

[1] State Key Laboratory of Hydraulics and Mountain River Engineering, Sichuan University, Chengdu 610065, China; zhang_wj@scu.edu.cn

[2] Numerical Terradynamic Simulation Group, The University of Montana, Missoula, MT 59812, USA; yonghong.yi@ntsg.umt.edu (Y.Y.), johnk@ntsg.umt.edu (J.S.K.)

[3] National Satellite Meteorology Center of China, Beijing 100081, China; luqf@cma.gov.cn

* Correspondence: songkech@lzb.ac.cn; Tel.: +86-28-8546-3699

Academic Editors: Javier Bustamante, Alfredo R. Huete, Patricia Kandus, Ricardo Díaz-Delgado, Richard Gloaguen and Prasad S. Thenkabail

Received: 21 January 2016; Accepted: 12 April 2016; Published: 18 April 2016

Abstract: Alpine wetlands in the Tibetan Plateau (TP) play a crucial role in the regional hydrological cycle due to their strong influence on surface ecohydrological processes; therefore, understanding how TP wetlands respond to climate change is essential for projecting their future condition and potential vulnerability. We investigated the hydrological responses of a large TP wetland complex to recent climate change, by combining multiple satellite observations and *in-situ* hydro-meteorological records. We found different responses of runoff production to regional warming trends among three basins with similar climate, topography and vegetation cover but different wetland proportions. The basin with larger wetland proportion (40.1%) had a lower mean runoff coefficient (0.173 ± 0.006), and also showed increasingly lower runoff level (-3.9% year^{-1}, $p = 0.002$) than the two adjacent basins. The satellite-based observations showed an increasing trend of annual non-frozen period, especially in the wetland-dominated region (2.64 day· year^{-1}, $p < 0.10$), and a strong extension of vegetation growing-season (0.26–0.41 day· year^{-1}, $p < 0.10$). Relatively strong increasing trends in evapotranspiration (ET) (~1.00 mm· year^{-1}, $p < 0.01$) and the vertical temperature gradient above ground surface (0.043 °C· year^{-1}, $p < 0.05$) in wetland-dominant areas were documented from satellite-based ET observations and weather station records. These results indicate recent surface drying and runoff reduction of alpine wetlands, and their potential vulnerability to degradation with continued climate warming.

Keywords: alpine wetlands; Tibetan Plateau; climate warming; hydrological response; Zoige

1. Introduction

High-altitude wetlands provide important hydrological and ecological functions to their populated regions and adjacent lowlands, as they regulate hydrological processes, mitigate flooding, minimize storm damage, supply water and provide critical ecological habitats [1]. These wetland functions are highly dependent on environmental and climatic factors that control either water recharge or discharge of wetland regions. Global highlands often experience stronger climate changes compared with adjacent regions [2,3]; therefore high-altitude wetlands may be more vulnerable to temperature and precipitation variations [4]. As wetlands develop and encompass aquatic environments with water present on or near land surface [1], the vulnerability of wetlands to climate change (mainly air temperature and precipitation) is dependent on how water recharge and discharge, and how associated wetland water balance responds to these changes [5]. Therefore, a better understanding of how the

hydrological functioning of high-altitude wetlands has responded to recent climate trends (particularly warming), is essential to project their resilience or vulnerability to future climate change [6–10].

The Tibetan Plateau (TP) is the source of the Mekong, Yangtze, Yellow, Indus, Brahmaputra and other major Asian rivers, where more than 110,000 km^2 of alpine wetlands have developed [11] and played a crucial role in regional hydrological regulation and water supply for much of the world's human population [6,12]. *In-situ* ground meteorological observations indicated distinct warming (>2.0 °C) over the whole Tibetan Plateau during the last half century, while precipitation did not change much over the same period [3,13,14]. In response to the warming, the length of annual non-frozen period (*i.e.*, the duration of days when the ground surface is not frozen) increased in most TP areas, indicated by both passive microwave remote sensing measurements [15] and model simulations [16]. These changes have likely promoted a longer potential growing-season and greater annual evapotranspiration rates [17] that may intensify surface water loss and soil drying. On the other hand, warming-induced deglaciation and permafrost thawing may contribute to the recent wetland expansion in the TP [8,18], and the discharge increases in some TP rivers during the last 40 years [7,10]. The understanding of how the above factors, with potentially contrasting effects on wetland development, interact and control hydrological sensitivity of the TP wetlands to climate warming is less studied [17,19,20], partly due to sparse *in-situ* observations in these remote alpine areas [12,17,21].

The Zoige Wetland, one of the largest alpine wetlands in the Tibetan Plateau, has experienced degradation in hydrology, soil and ecological conditions, likely due to the impact of human activities and climate change since the 1970s [17,22]. This wetland accounts for ~30% of winter runoff production of the upper Yellow River (uYR) [23], and is the largest peat reserve in China (containing ~0.50 Pg C in the upper 0–3 m soil layer) [22,24]. However, during the last 50 years, the surface water depth of the Zoige Wetland has greatly declined with wetland shrinkage [6,17,25], and typical wetland species have been replaced by mesophytes in some severely degraded areas [19,26]. Previous studies attributed the wetland degradation mainly to ditching and associated drainage impacts from the 1970s [17], as well as over-grazing [6,27], which may underestimate the hydrological sensitivity of these alpine wetlands to recent climate warming. Investigating how the Zoige Wetland responds to warming will improve regional projections of hydrological and ecological responses of the TP wetlands to future climate change.

The main objective of this study is therefore to investigate hydrological response of the Zoige Wetland to climate warming by exploiting multiple satellite observations as well as *in-situ* hydro-meteorological records extending from 1985 to 2007. The Zoige Wetland provides a regional case study of the larger Tibetan Plateau wetland system. Two Zoige basins with different wetland proportions were analyzed in parallel to investigate the hydrological responses of alpine wetlands to recent climate warming. The two basins were also compared against the upper Yellow River basin, which has similar climate conditions but negligible wetland coverage, to understand the difference in the hydrological responses of alpine wetlands and non-wetlands in the TP to regional climate trends.

2. Data and Methodology

2.1. Study Area

The Zoige wetland complex lies in the eastern Tibetan Plateau, and consists of many wetland patches within the Zoige Basin (102–103°E, 33–34°N, ~20,000 km^2) [28] (Figure 1). The Zoige wetland complex has a characteristic alpine wet and cold climate [22], with annual mean air temperature (AMT) of 1.62 °C and annual total precipitation (ATP) of 640 mm. The upper Yellow River (uYR) runs through this basin from Qiujima to Maqu. Two major rivers run through the Zoige Basin, *i.e.*, the White River (WR) and the Black River (BR), and flow northward to the Yellow River. The uYR basin has a similar climate as the Zoige region with AMT of 0.32 °C and ATP of 550 mm. The areas of the BR and WR basins are ~8061 km^2 and ~5358 km^2, respectively, and the area of the uYR basin

above Maqu is ~70,251 km^2 (with the WR and BR basins excluded). The three basins have a mean elevation of 4200 ± 394 m (mean ± SD), 3550 ± 148 m and 3700 ± 187 m (a.s.l.) for uYR, BR and WR, respectively. However, these basins are not significantly different in topographical variations, with mean slopes of 10.4° ± 8.3° (uYR), 8.9° ± 7.1° (BR) and 11.6° ± 8.4° (WR), respectively. General physical characteristics of the three basins are summarized in Table 1.

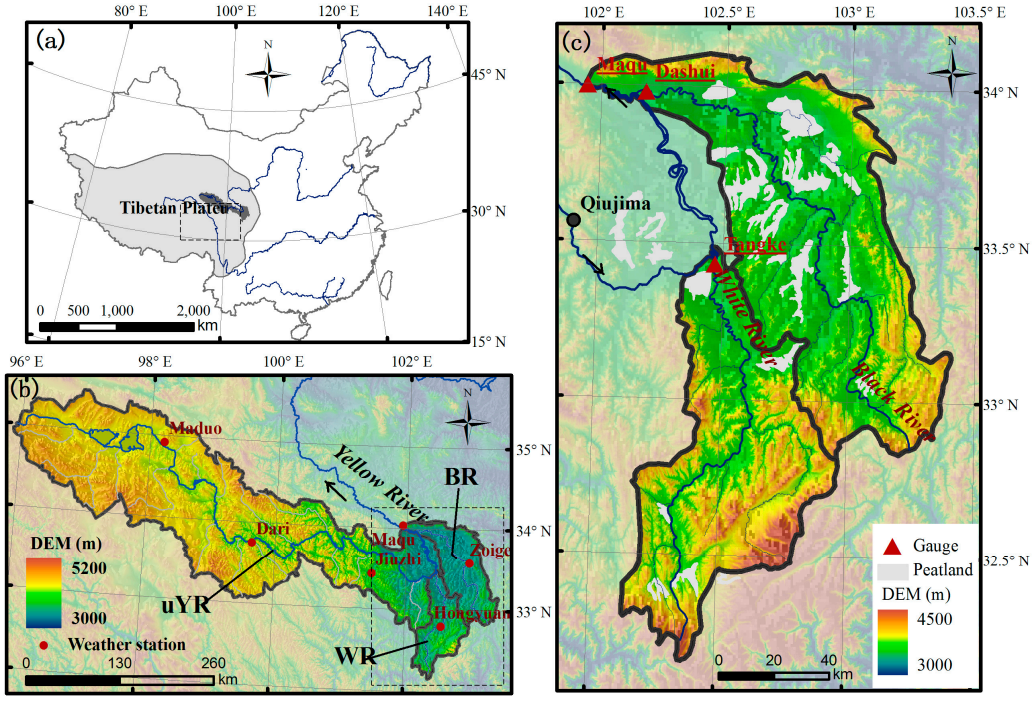

Figure 1. The location and terrain of the upper Yellow River (**a**,**b**) and Zoige Wetland complex (**c**). The six weather stations (Maduo, Dari, Jiuzhi, Hongyuan, Zoige and Maqu) and three hydrological gauges (Maqu on the uYR, Tangke on the WR, and Dashui on the BR) used in the study are shown in Figure 1b,c, respectively.

Table 1. General characteristics of the three Tibetan Plateau basins in this study, including the upper Yellow River (uYR), White River (WR) and Black River (BR) basins. Annual mean air temperature and annual total precipitation are abbreviated as AMT and ATP, respectively.

Basin	Area (km^2)	Elevation Mean ± SD (m)	Slope Mean ± SD (°)	AMT (°C)	ATP (mm)	Gauge	Location	Wetland Proportion
uYR *	70,251	4200 ± 394	10.4 ± 8.3	0.32	550	Maqu	33.97°N 102.08°E	1.8%
WR	5358	3700 ± 187	11.6 ± 8.4	1.62	640	Tangke	33.42°N 102.46°E	17.1%
BR	8061	3550 ± 148	8.9 ± 7.1			Dashui	33.98°N 102.27°E	40.1%

* with the WR and BR basins excluded.

There is a large difference in wetland coverage among the two Zoige basins and uYR basin. Over 75% of the Zoige wetland complex is distributed within the WR (16.6%) and BR (59.9%) basins, and wetlands account for 17.1% and 40.1% of total area of the two basins, respectively, while the wetland proportion is negligible in the uYR basin (~1.8%, with the WR and BR basins excluded). The Zoige Wetland vegetation is dominated by helophyte species (*Carex mulliensis*, *Carex meyeriana* and *Carex lasiocarpa*) as well as some hydrophyte species (*Potamogeton* sp. and *Utricularia intermedia*) [22,29].

The upper peat soil layer in the Zoige Wetland ranges from 1 to 10 m depth depending on local geomorphology [22,24]. Except for the difference in wetland areas, the three river basins are mainly covered by alpine meadow dominated by *Kobresia tibetica* (Figure 2; [30]).

2.2. In-Situ Data

In-situ hydro-meteorological observations were used to examine annual and seasonal variations in surface climate and hydrology during the 1985–2007 study period. Due to similar climate, topographical and vegetation conditions, except for wetland coverage differences between the uYR and Zoige basins, hydrological responses in the WR and BR basins were analyzed against the uYR region to provide a better understanding of potential warming-induced changes in surface hydrology. Three hydrological gauges were used in this study (Figure 1c), including Dashui, Tangke and Maqu at the outlets of the BR, WR and uYR basins, respectively. The discharge observations were continuously available at a daily time step during the overlapping period of 1985–2007, as provided by the Yellow River Conservancy Commission. We excluded the runoff contributioin of the Zoige wetland complex from the discharge observation of the uYR by deducting the WR and BR discharges from Maqu gauge records. Variations in air temperature and precipitation over the Zoige region were evaluated using daily meteorological records from Hongyuan (3492 m a.s.l.) and Zoige (3440 m a.s.l.) weather stations, while meteorological records from Maduo (4272 m a.s.l.), Dari (3968 m a.s.l.), Jiuzhi (3629 m a.s.l.) and Maqu (3471 m a.s.l.) weather stations were used to indicate climate variation over the uYR basin (Figure 1b). Details about the weather stations are summarized in Table 2. As surface ground temperature is closely associated with changes in surface moisture and thermal conditions, we used the vertical temperature gradient at the ground surface (~0 cm depth) measured at the weather stations to evaluate potential differences in warming-induced surface changes between wetlands and non-wetlands. The ground surface temperature is measured using an earth thermometer with each half of its bulb located in air and below the soil surface in an area with bare, loose soil [31]. Pan evaporation measurements at the weather stations (1982–2001) were used to characterize changes in open water evaporation associated with variations in surface climate conditions, and as an *in-situ* measurement reference on evaporative water losses in conjunction with the satellite-based ET estimates.

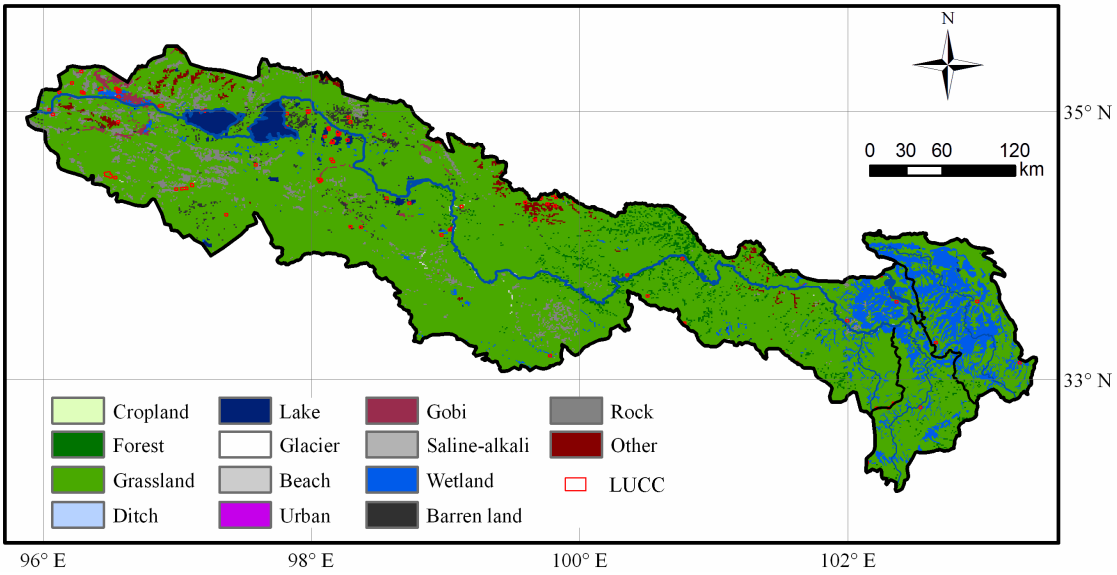

Figure 2. The land cover map of the uYR basin in 1985 derived from a satellite-based Land-use and Land cover Dataset of China [32]. The red polygons indicate areas with land use and cover changes larger than 1 km^2 occurring during the period of 1985–2005.

Table 2. Characteristics of the *in-situ* weather stations used for climate trend detection in the three TP basins. AMT denotes annual mean air temperature, while ATP denotes annual total precipitation.

Site	Lon	Lat	Elevation (m)	Basin	AMT (°C)	ATP (mm)
Maduo	98.22°N	34.92°E	4272	uYR	−3.28	329.8
Dari	99.65°N	33.75°E	3968	uYR	−0.52	546.6
Jiuzhi	101.48°N	33.43°E	3629	uYR	1.10	721.2
Maqu	102.08°N	34.00°E	3471	uYR	1.87	586.0
Zoige	102.97°N	33.58°E	3440	BR	1.47	625.9
Hongyuan	102.55°N	32.80°E	3492	WR	1.78	722.0

2.3. Remote Sensing Measurements

Land use and cover change (LUCC) exerts a large impact on the surface hydrology due to its influence on surface albedo and net solar radiation, evapotranspiration (ET) and soil moisture [7]. We used the satellite-based Land-use and Land-cover Dataset of China (LUCC-China; [32]) to examine recent land use and cover changes in the study area. This dataset was produced by interpreting visual-infrared satellite images mainly acquired by the Landsat Thematic Mapper, available at a 1-km resolution for years 1985, 1995, 2000, 2005 and 2010 [32]. This dataset identified six major land cover classes in China (*i.e.*, cropland, woodland, grassland, water body, built-up land and unused land) and 25 subclasses; the accuracy of the six major land cover classes was reported to be above 94.3%, while the overall accuracy of the 25 subclasses was above 91.2% [32]. In the study, hydrological gauge records covered the period from 1985 to 2007, so we selected the land cover maps for 1985 and 2005 to quantify land use and cover changes over the study area during the 1985–2007 study period (Figure 2).

The landscape freeze/thaw (F/T) status derived from satellite microwave observations has been shown to be closely linked with surface energy budget, hydrological activity and vegetation growing-season dynamics due to strong control of surface F/T status on vegetation growth and hydrological cycles [17,33]. In this study, a global F/T Earth System Data Record (FT-ESDR; [34]) derived from satellite passive microwave remote sensing observations was used to assess variations in land surface F/T status and its association with surface hydrology over the study area. The FT-ESDR dataset is produced by identifying surface F/T status derived from a temporal change classification of 37 GHz daily brightness temperature (Tb) in relation to reference frozen and unfrozen Tb conditions. The F/T status of land surface is derived from calibrated overlapping Tb records from the Scanning Multichannel Microwave Radiometer and Special Sensor Microwave Imager [35]. This F/T dataset has a 25-km spatial resolution and daily temporal fidelity that was used to determine the primary thaw day in the spring, primary frozen day in the fall and the annual non-frozen period for each year of the 1985–2007 study period. The primary thaw day was determined as the first day when 12 out of 15 consecutive days from January through June were classified as non-frozen, while the primary frozen day was determined as the first day when 12 out of 15 consecutive days from September through December were classified as frozen [34]. The non-frozen period was defined as the number of days between the primary thaw and primary frozen dates for each calendar year.

Vegetation exerts strong controls on surface hydrology mainly through regulating surface evapotranspiration (ET) and vegetation phenology, including growing-season timing and duration, which has important controls on vegetation activities and surface energy/water fluxes [2,36]. In this study, we used the satellite observed normalized difference vegetation index (NDVI) from the third generation Global Inventory Modeling and Mapping Studies (GIMMS3g) dataset to detect variations in vegetation phenology during the study period. The GIMMS3g NDVI record has an 8-km spatial resolution and a 15-day temporal interval, and was assembled from different NOAA Advanced Very High Resolution Radiometer (AVHRR) records accounting for various deleterious effects including calibration loss, orbital drift and volcanic eruptions [37]. The dynamic threshold method, which defined the threshold of vegetation growing-season onset and offset as 25% of the seasonal NDVI amplitude based on the multi-year average [2,38], was used to derive growing season onset, offset

and duration [2,14,38]. Prior to the phenology analysis, the NDVI time series were filtered using the double logistic method from the Timesat Tool to remove outliers and fill data gaps [38].

We also adopted a global evapotranspiration (ET) dataset upscaled from global FLUXNET tower observations to examine the spatial and temporal variations in surface water loss through ET over the Zoige and uYR basins [39,40]. This global half-degree dataset of water and energy fluxes (1982–2011) was produced by spatially upscaling FLUXNET observations with machine learning techniques and model tree ensembles combining observations of ancillary climate datasets, tower-based eddy-covariance measurements and satellite-based vegetation observations [39]. The mean annual ET (247.2 $\pm$ 55.0 mm) at a Tibetan Plateau site (92.90°E, 34.75°N, ~4600 m a.s.l.) in 2007 and 2008 estimated by this dataset generally agreed with the *in-situ* lysimeter-based ET observations (288.4 $\pm$ 36.1 mm), indicating favorable accuracy of the global ET dataset for the eastern alpine Tibetan Plateau [41]. Therefore, this dataset was used to compare the difference in surface ET variations among the basins in the study area.

2.4. Data Analysis

Linear regression analysis was used to detect regional trends in climate and hydrological variables, including satellite-based records at both annual and seasonal scales during the study period; the significance level of each regression slope was examined using the *F*-test metric. Seasonal differences in hydrological variations were examined by aggregating basin stream gauge discharges during the warm season (from May to September) and cold season (from October to April). For consistency in inter-basin comparisons, stream discharges were normalized by the multi-year average discharge within each basin. To examine relations between climate variables and basin discharges, daily air temperature and precipitation were also temporally aggregated at annual and seasonal (*i.e.*, warm and cold seasons) scales from 1985 to 2007. Though both annual air temperature and precipitation decrease with elevation increase at respective gradients of -0.58 °C ($p < 0.01$) and -38 mm ($p < 0.05$) per 100 m within the study area, our initial analyses did not indicate a significant correlation between climatic trends and station elevations. This was partially supported by satellite-observed land surface temperatures over the TP within the 3400–4200 m elevation range [42] and the analysis of altitudinal influences on precipitation in the TP [43]. Therefore, we did not adjust for elevation effects on the trends of either air temperature or precipitation records reported here. We also analyzed trends in the satellite-based annual non-frozen period, NDVI defined growing-season length and ET records to detect variations in surface conditions and associated climate impacts across the study area (including uYR, WR and BR basins), which provide spatially continuous regional observations across the domain in context with detailed measurements of river discharge and surface meteorology from the *in-situ* station network.

3. Results

3.1. Changes in Surface Climate and Land Cover Conditions

The *in-situ* weather station observations indicated that both the Zoige and uYR regions experienced significant warming trends during the 1985–2007 study period as shown in Table 3 (Zoige: 0.058 °C· year^{-1}; uYR: 0.065 °C· year^{-1}, both $p < 0.05$), while no significant trends were detected in either annual ($p > 0.55$) or seasonal ($p > 0.10$) precipitation in these regions (Table 3). The Zoige and uYR regions showed similar inter-annual variations in air temperature (Ta: $R = 0.98$, $p < 0.001$) and precipitation (P: $R = 0.91$, $p < 0.001$). The Zoige wetland complex also showed 1.47 °C and 2.31 °C warmer mean Ta during respective warm and cold seasons as a consequence of being approximately 600 m lower in elevation than the uYR (Table 3). More annual precipitation fell in the Zoige region (644.6 $\pm$ 62.4 mm) due to atmospheric water vapor conveyed to this region more easily [13], in contrast with annual precipitation of 545.9 $\pm$ 58.6 mm in the uYR basin (Table 3). In both regions, about 80% of annual precipitation fell during the warm season.

Table 3. Climate trends of the Zoige Basin and the uYR basin from 1985 to 2007 represented by weather station observations (Ta, air temperature, °C; Ta trend: °C· year^{-1}; precipitation trend: mm· year^{-1}).

Climatic Variable	Period	Zoige		uYR	
		Mean ± SD	Trend	Mean ± SD	Trend
Air temperature	Annual	1.71 ± 0.56	0.058 *	−0.21 ± 0.64	0.065 *
	Warm-season	8.82 ± 0.53	0.051 **	7.45 ± 0.52	0.054 **
	Cold-season	−3.42 ± 0.69	0.052 **	−5.73 ± 0.84	0.061 **
Precipitation	Annual	644.6 ± 62.4	−0.151	545.9 ± 58.6	1.170
	Warm-season	512.1 ± 57.3	−1.169	447.2 ± 53.1	1.110
	Cold-season	132.6 ± 34.6	1.018	98.7 ± 22.9	0.061

Note: ** denotes the significance level $p < 0.01$, * denotes the significance level $p < 0.05$ and SD denotes the temporal standard deviation.

Our analysis showed negligible changes in the land cover of the study area from 1985 to 2005. As indicated by the LUCC-China dataset in 1985, grasslands and wetlands accounted for more than 85% of the three basins (Figure 2 and Table 4). Grassland was the dominant land cover type in the study region, while the areal proportions of wetland coverage were quite different among the three basins, *i.e.*, 40.1% in the BR, 17.1% in the WR and only 1.8% in the uYR (with the WR and BR basins excluded), as summarized in Table 4. During the 1985–2005 study period, less than 0.14% (~110 km^2) of the whole study area experienced land use and cover change (mainly converting from grasslands to other land cover categories as shown in Table 5). As indicated by Figure 2 and Table 5, most of the land use and cover change occurred in the upstream areas of the uYR, with only 3 km^2 and 2 km^2 of land cover conversion occurring in the BR and WR basins, respectively. The net changes in the forest and lake cover (about 6 km^2 and 15 km^2, respectively) were less than 1% of the corresponding areas of these land cover types in the uYR basin. Therefore, the hydrological influence of land use and cover changes was assumed negligible in the study, particularly in the Zoige wetland.

Table 4. Reference land cover characteristics in the uYR, BR and WR basins in 1985 derived from the satellite-based Land-use and Land cover Dataset of China [32].

Land Cover	uYR	BR	WR	Land Cover	uYR	BR	WR
Grassland	84.76%	58.79%	80.40%	Gobi desert	0.80%	0.11%	0.00%
Rock	4.85%	0.04%	0.00%	Beach	0.26%	0.10%	0.02%
Forest	2.36%	0.64%	2.35%	Ditch	0.07%	0.04%	0.09%
Lake	2.17%	0.16%	0.02%	Snow	0.01%	0.00%	0.00%
Wetland	1.80%	40.10%	17.10%	Saline-alkali	0.00%	0.00%	0.00%
Other	1.66%	0.00%	0.00%	Cropland	0.00%	0.00%	0.02%
Barren land	1.27%	0.00%	0.00%	Urban	0.00%	0.02%	0.00%

Table 5. The area statistics of land use and cover change in the study area from 1985 to 2005 indicated by the satellite-based Land Use and Land Cover Dataset of China (km^2). Most of the land use and cover changes occurred in upstream areas of the uYR basin, with only 3 km^2 and 2 km^2 of land cover conversion occurring in the BR and WR basins, respectively.

Land Cover		Conversion Area (km^2)			Land Cover		Conversion Area (km^2)		
From	To	uYR	BR	WR	From	To	uYR	BR	WR
Grassland	Forest	4	0	0	Lake	Grassland	11	1	0
	Ditch	1	0	0		Beach	4	0	0
	Lake	3	0	0		Gobi	2	0	0
	Beach	8	0	0	Gobi desert	Grassland	1	0	0
	Urban	2	0	0		Gobi	2	0	0

Table 5. *Cont.*

Land Cover		Conversion Area (km²)			Land Cover		Conversion Area (km²)		
From	**To**	**uYR**	**BR**	**WR**	**From**	**To**	**uYR**	**BR**	**WR**
	Gobi	30	1	1	Forest		8	1	1
	Saline-Alkali	1	0	0	Beach		3	0	0
	Barren land	4	0	0	Barren land	Grassland	4	0	0
	Rock	1	0	0	Rock		5	0	0
	Other	1	0	0	Other		10	0	0
Sum		55	1	1	Sum		50	2	1

3.2. Changes in Hydrological Responses

The BR basin with the largest wetland proportion (40.1%) showed extremely low runoff production compared with the WR and uYR basins during the 1985–2007 record. Despite having a larger basin area, the BR basin had relatively lower discharge in both the warm-season (43.8 ± 18.3 $m^3 \cdot s^{-1}$) and cold-season (12.1 ± 3.3 $m^3 \cdot s^{-1}$) compared with the WR basin, which had larger respective seasonal discharges of 92.2 ± 25.4 $m^3 \cdot s^{-1}$ and 22.9 ± 6.2 $m^3 \cdot s^{-1}$ (Table 6). This was likely due to larger water retention capacity [44] and higher evapotranspiration rates in areas with larger wetland proportion, as indicated by the satellite-based ET estimates (BR: 458 ± 97 mm$\cdot$ year^{-1}; WR: 438 mm $\pm$ 48 year^{-1}). Therefore, the annual runoff coefficient (discharge/precipitation) of the BR basin (0.173 ± 0.006) was much smaller than that of the WR basin (0.475 ± 0.008), with the intermediate runoff production efficiency for the uYR region (0.271 ± 0.003).

Table 6. River discharge trends from the Zoige basins and uYR from 1985 to 2007 at annual and seasonal scales (warm season, from May to September; cold season, from October to April). The slopes of original and normalized (Norm.) discharges are in m^3 $s^{-1}\cdot$ year^{-1} and year^{-1}, respectively.

	Discharge	**WR**	**BR**	**uYR**
Annual	Original, $m^3 \cdot s^{-1} \cdot$ year^{-1}	−0.74	−0.97 **	−2.07
	Norm., year^{-1}	−1.3%	−3.5% **	−0.6%
Warm season	Original, $m^3 \cdot s^{-1} \cdot$ year^{-1}	−1.86 *	−1.72 **	−3.47
	Norm., year^{-1}	−2.0% *	−3.9% **	−0.7%
Cold season	Original, m^3 $s^{-1}\cdot$ year^{-1}	0.40 *	−0.21 *	−0.65
	Norm., year^{-1}	1.7% *	−1.7% *	−0.5%

Note: ** denotes the significance level $p < 0.01$, * denotes the significance level $p < 0.05$.

The hydrological trends in the BR basin were also different from the adjacent WR and uYR basins during the study period (Figure 3). The annual discharge measurements showed a significant decline (-0.97 m^3 $s^{-1}\cdot$ year^{-1}, $p < 0.01$) in the BR basin, while no significant ($p > 0.10$) trends were observed in the WR and uYR basins (Table 6). Warm-season discharge of the WR and BR basins showed similar decreasing trends in absolute magnitude (~-1.80 $m^3 \cdot s^{-1}$ year^{-1}, $p < 0.05$; Table 6), partially due to a strong warming trend (~0.051 °C$\cdot$ year^{-1}, $p < 0.01$) and a non-significant decreasing trend in precipitation (-1.169 mm$\cdot$ year^{-1}, $p = 0.81$). However, in terms of normalized warm-season discharges, the decrease rate of the BR basin (-3.9% year^{-1}, $p < 0.01$) was nearly twice the rate of the WR (-2.0% year^{-1}, $p = 0.02$). In contrast, during the cold-season, the discharge measurements showed opposite trends in the two basins (WR: 0.40 m^3 $s^{-1}\cdot$ year^{-1}, 1.7%, $p < 0.05$; BR: -0.21 m^3 $s^{-1}\cdot$ year^{-1}, -1.7%, $p < 0.05$) (Table 6) despite a slightly increasing precipitation trend (1.018 mm$\cdot$ year^{-1}, $p > 0.10$). The slight increase in cold-season runoff from the WR basin was likely caused by winter precipitation increase in its mountainous upper reach (over 4000 m a.s.l.). Therefore, the WR basin showed a much weaker decreasing trend in annual discharge (-1.3% year^{-1}, $p = 0.10$) than the BR basin (-3.5% year^{-1}, $p < 0.01$). As for the uYR basin, no significant trends ($p > 0.35$; Table 6) were observed in

either annual or seasonal discharge during the study period despite similar warming trends, likely due to a non-significant increasing trend in precipitation, particularly during the warm-season (Table 3).

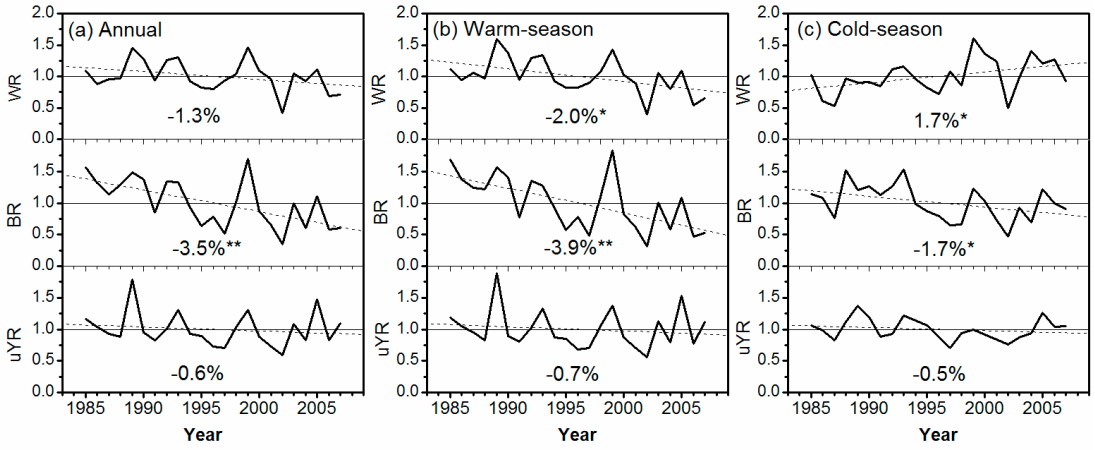

Figure 3. The normalized annual (**a**); warm season (from May to September) (**b**); and cold season (from October to April) (**c**) discharges of the WR, BR and uYR basins from 1985 to 2007. The dot dash lines indicate the regression lines of the discharge series. The numbers at panel bottom are the linear-regression slopes for the normalized discharges, while ** and * denote the significance levels $p < 0.01$ and $p < 0.05$, respectively.

3.3. Changes in Non-Frozen Period and Growing-Season Length

The FT-ESDR results showed different trends in surface F/T status among the three basins (Figure 4). Spatial variations in the primary thaw (frozen) day were congruent with the regional topography, with a general delay (advance) in the primary thaw (frozen) day at higher elevations in the study area (Figure 4a,c). The resulting annual non-frozen period also became shorter with increasing elevation (Figure 4e). However, regional variations in F/T trends were less related to the elevation gradient than regional climate changes (Figure 4b,d,f). The primary thaw day advanced significantly at a rate of -0.85 day$\cdot$ year^{-1} ($p < 0.01$) in the BR basin due to continuous spring warming (0.052 °C$\cdot$ year^{-1}, $p < 0.01$), but advanced with a relatively weaker trend in the WR basin (-0.60 day$\cdot$ year^{-1}, $p = 0.13$), while the uYR region showed no significant thaw trend (-0.41 day$\cdot$ year^{-1}, $p = 0.35$). On the other hand, all three basins showed consistent trends toward delayed seasonal freezing, but with relatively larger rates in the Zoige basins (BR: 0.95 day$\cdot$ year^{-1}, $p < 0.05$; WR: 1.10 day$\cdot$ year^{-1}, $p < 0.10$; uYR, 0.57 day$\cdot$ year^{-1}, $p < 0.10$) coinciding with a strong fall warming trend (0.065 °C$\cdot$ year^{-1}, $p < 0.01$). Therefore, the two Zoige basins showed much stronger increasing trends in the annual non-frozen period (BR: 2.64 day$\cdot$ year^{-1}, $p < 0.10$; WR: 2.43 day$\cdot$ year^{-1}, $p < 0.10$) than the uYR basin (0.90 day$\cdot$ year^{-1}, $p = 0.18$).

Similar to the response of surface F/T status to spring and fall warming, vegetation phenology derived from the GIMMS3g NDVI record also showed an advancing trend in spring canopy green-up and a delaying trend in fall canopy senescence over the 1985–2007 study period (Figure 5). In contrast to the primary thaw day trend, the advancing trend in spring onset was relatively weaker in the two wetland-dominated basins (~-0.15 day$\cdot$ year^{-1}, $p > 0.21$) than in the uYR region (-0.26 day$\cdot$ year^{-1}, $p = 0.05$), while the delaying trend in fall canopy senescence was similar in all three basins (0.12–0.16 day$\cdot$ year^{-1}, $p < 0.19$) and consistent with the strong delaying trend in surface freezing in the fall (Figure 4d). The study area therefore experienced an increasingly longer growing-season (0.26–0.41 day$\cdot$ year^{-1}, $p < 0.10$) over the study period, especially in the uYR region (0.41 day$\cdot$ year^{-1}, $p < 0.001$), but with no significant increase in growing-season NDVI ($p > 0.80$; Figure 6c).

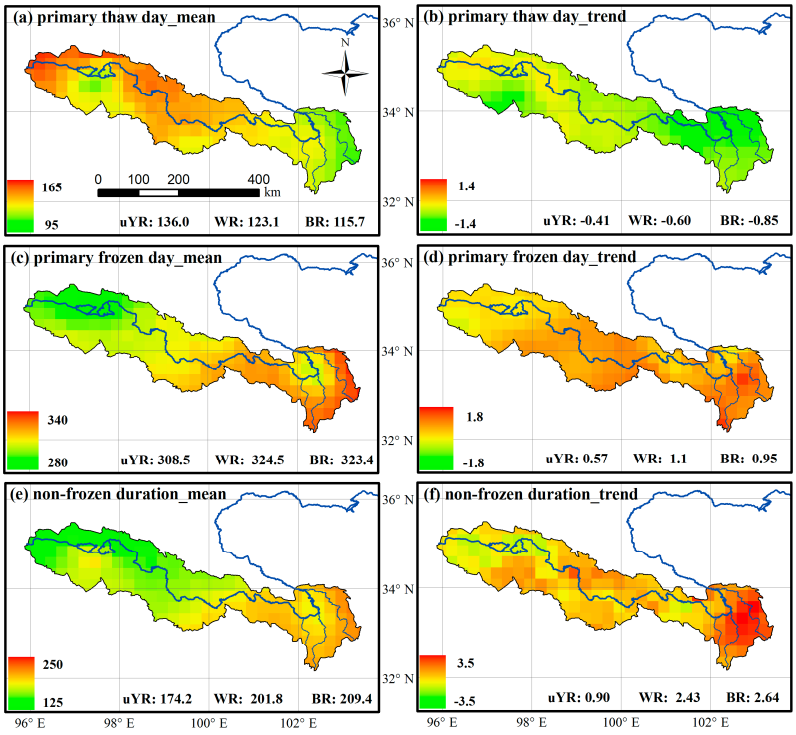

Figure 4. The means and trends (day· year^{-1}) of three freeze-thaw metrics based on the satellite FT-ESDR dataset [35] during the period from 1985 to 2007: (**a**,**b**) means (the day of year, DOY) and trend (day· year^{-1}) of primary thaw day in the spring (*i.e.*, the timing when the surface begins to thaw); (**c**,**d**) means (DOY) and trend (day· year^{-1}) of primary frozen day in the fall (*i.e.*, the timing when the surface begins to freeze); and (**e**,**f**) mean (days) and trend (day· year^{-1}) of annual non-frozen period (*i.e.*, the number of days between primary thaw and frozen dates).

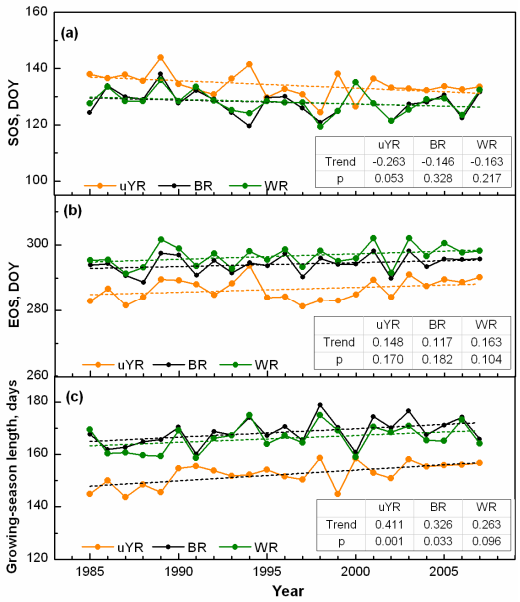

Figure 5. The trends in three phenological metrics derived from the GIMMS3g NDVI dataset during the period from 1985 to 2007 in the TP study areas, including, (**a**) start of growing-season (SOS, in day of year, DOY); (**b**) end of growing-season (EOS, in DOY) and (**c**) annual growing-season length (in days).

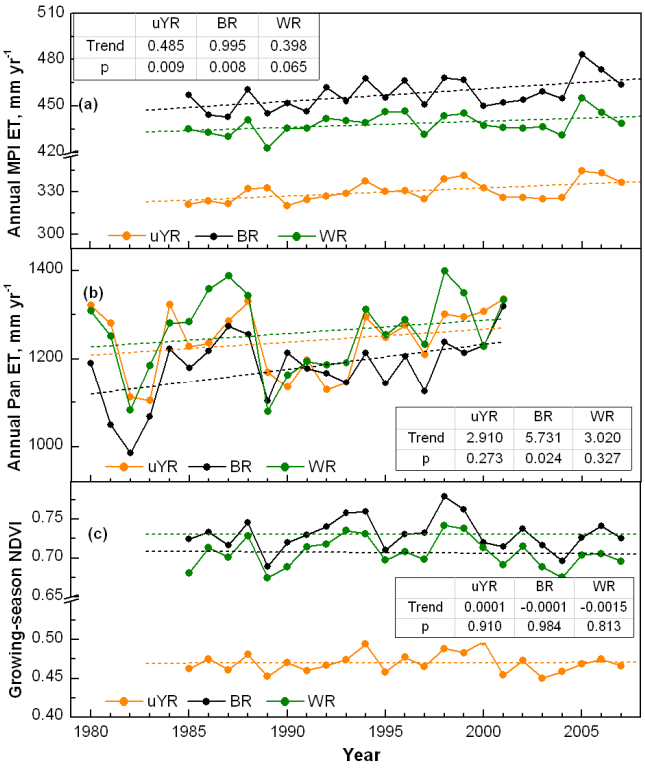

Figure 6. The annual ET (**a**,**b**) and growing-season Normalized Difference Vegetation Index (NDVI) (**c**) in the BR, WR and uYR basins. (**a**) MPI ET was derived from a global ET dataset upscaled from FLUXNET tower observations [39], while the reference ET (**b**) was obtained from pan evaporation measurements within the study domain. The NDVI record was derived from the GIMMS3g dataset. The trends were calculated for different periods (*i.e.*, 1985–2007 in panels (**a**) and (**c**), and 1980–2001 in panel (**b**)) due to data availability constraints.

3.4. Changes in Surface Evapotranspiration and Thermal Conditions

Both the upscaled ET dataset [39] and *in-situ* pan evaporation measurements indicated more water loss from the wetland-dominant regions relative to adjacent areas in the study domain (Figure 6). The upscaled ET dataset indicated that the increasing rate of ET in the BR basin (0.995 mm· year^{-1}, $p < 0.01$) from 1985 to 2007 was more than twice that of the uYR (0.485 mm· year^{-1}, $p < 0.01$) and WR (0.398 mm· year^{-1}, $p = 0.07$) basins. These findings were partially supported by the *in-situ* pan evaporation reference observations. During the overlapping period (1985–2001), the pan evaporation measurements and satellite-based ET dataset both indicated stronger positive ET trends in the wetland-dominated BR basin than in the WR and uYR region. The data also showed that pan evaporation representing an open water surface reference is much larger than the MPI ET estimates representing the regional landscape. Large uncertainty is likely associated with the MPI ET dataset in this area due to very few flux tower measurements representing TP conditions in the MPI ET record. However, similar positive trends in the ET and pan evaporation data were consistent with regional climate warming. The strong increasing trends in annual ET and regional differences in the magnitude of the ET trends among the three basins were not likely caused by the changes in surface vegetation cover as the LUCC-China dataset did not show distinct changes in land use and cover during the study period (Figure 2).

The *in-situ* weather station observations indicated an increasing trend in the vertical temperature gradient (Tdiff) between the ground surface and overlying air in the wetland-dominated region during both the warm and cold seasons (Figure 7b,d). The Tdiff increase is likely associated with climate warming-induced changes in surface thermal and moisture conditions. As climate warming

tends to result in drier ground surface and thus warmer ground surface, the increasing vertical Tdiff gradient above ground surface probably may reflect a trend toward the relatively drier ground surface conditions due to warming. Despite similar warming trends in the Zoige and uYR regions, Tdiff showed strong spatial variations across weather stations likely due to the heterogeneities in land surface, soil, topography and climate. Stations in the Zoige region demonstrated a larger increasing trend in Tdiff during the warm season (0.043 °C· year^{-1}, $p < 0.05$). Other stations in the study region and adjacent areas showed a much weaker increase or no significant change in Tdiff over the study period (−0.03~0.025 °C· year^{-1}, $p > 0.10$), likely due to different responses of land surface moisture status to climate warming at higher elevations [45]. However, regional differences in cold-season Tdiff trends between the Zoige and uYR were relatively small (Figure 7d). The stations also showed a generally larger temperature gradient during the warm-season (~3–5 °C) than in the cold-season (<3 °C).

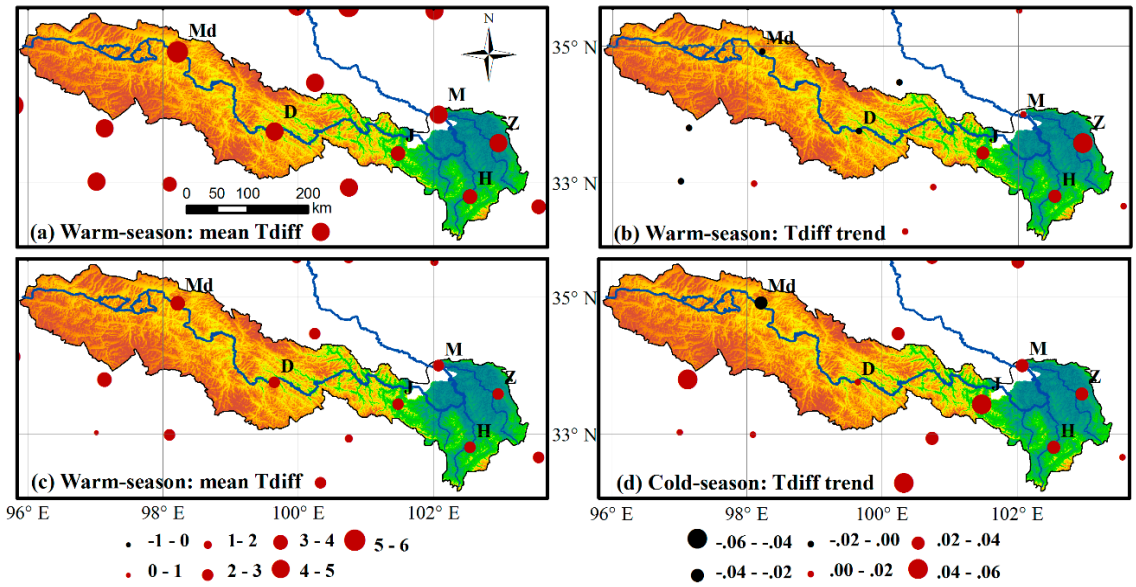

Figure 7. The means (°C) and trends (°C· year^{-1}) of the surface air-ground vertical temperature difference (Tdiff) based on *in-situ* weather station measurements during the 1985–2007 period: (**a**,**b**) warm-season (from May to September); and (**c**,**d**) cold-season (from October to April). Red (black) dots indicate positive (negative) Tdiff mean or trend with the magnitudes proportional to the symbol size. The weather stations used include M (Maqu), Z (Zoige), H (Hongyuan), J (Jiuzhi), D (Dari) and Md (Maduo).

4. Discussion

Our results show a strong decreasing trend in annual river discharge of a wetland-dominated basin in the eastern Tibetan Plateau in response to recent climate warming from 1985 to 2007. Difference in discharge trends among the three basins is attributed to the strong sensitivity of hydrological responses of alpine wetlands to warming, which may induce larger positive ET trends in wetland areas. The increasingly larger ET tends to result in less water available for discharge due to extending growing-season length and increasing vertical temperature gradient between the ground surface and air.

4.1. Climate Warming and Its Impact on Hydrological Response of the Zoige Wetland

Our results show persistent warming (>0.058 °C· year^{-1}, $p < 0.05$) without corresponding significant precipitation increase in the Zoige wetland complex and adjacent region. The climate variability has induced strong changes in seasonal freeze/thaw processes, and surface moisture

and temperature conditions indicated by both *in-situ* and satellite-based measurements. These changes likely explain the different responses of runoff production among the basins with different wetland proportions.

A much stronger increase in the non-frozen period and annual ET over the BR basin despite in a similar warming trend as the uYR and WR basins (Figure 6 and Table 3), could explain the relatively stronger discharge decline for the BR basin (Figure 3). In response to strong warming trends in spring (0.052 °C· year^{-1}, $p < 0.01$) and fall (0.065 °C· year^{-1}, $p < 0.01$), the annual non-frozen period increased significantly in the study area from 1985 to 2007 (0.90–2.64 day· year^{-1}, $p < 0.19$), with the strongest increase in the BR basin (Figure 4). The satellite NDVI dataset also indicated a longer vegetation growing-season in the study area (Figure 5: 0.263–0.411 day· year^{-1}, $p < 0.10$) coincident with regional climate warming and a longer non-frozen period. The trends in the non-frozen period indicated by the FT-ESDR and the growing-season length trends derived from the NDVI record show some inconsistencies in both wetland-dominated and non-wetland areas. This may imply that the microwave-based F/T retrievals are more sensitive to changes in surface soil moisture conditions [15,34], which likely differ between the wetland and non-wetland areas. Generally, wetlands develop and exist in aquatic or semi-aquatic environments with relatively weak or negligible water deficit, while the hydrological and ecological functions of wetland are maintained by characteristically slow and low runoff production due to its large water holding capacity [1]. A longer non-frozen period and associated climate warming may promote additional ET-related water losses [17], particularly in wetland-dominated areas with a more persistent water supply and relatively lower evaporative resistance, which may account for the apparent stronger sensitivity of hydrological responses in these alpine wetlands. The satellite-based ET dataset and the *in-situ* pan evaporation measurements both indicated a much larger magnitude and increasing trend in surface ET in the wetland-dominated basin (*i.e.*, BR) than the other adjacent basins with similar climate trends but less wetland coverage (*i.e.*, uYR and WR), consistent with relatively stronger wetland hydrological sensitivity.

Our results indicate that recent climate warming may also change the surface moisture and thermal gradients by altering surface energy and water balance. Warming-induced evaporative water loss from the ground surface may intensify surface soil drying, leading to larger temperature gradients due to a lower heat capacity and thermal buffering from drier soils, and relatively stronger effects in wetland-dominated areas [26]. The *in-situ* surface weather stations showed a much stronger increasing trend in the vertical temperature gradient between surface air and ground (0 cm) in the wetland-dominated region (Figure 7), which is likely caused by surface water loss in this area (Figure 6). The increasing trend in vertical air-surface thermal gradient in the Zoige Wetland is consistent with a previous report for adjacent wetland regions [46]. Relatively large sensitivity of wetlands to recent climate change was also found to cause stronger surface warming in a central European wetland than in adjacent areas [47]. Therefore, continued warming without corresponding precipitation increase may expose alpine wetlands in the TP to potential degradation because further water losses may alter the regional water balance to the point where the water table is below a minimum threshold necessary to maintain wetland persistence, extent and integrity.

4.2. Impact of Human Activities on the Hydrology Response of the Zoige Wetland

In contrast with previous studies [17,19,26], our study results indicate that direct human management impacts including ditching, drainage and land use change played limited roles in the observed hydrological changes of the Zoige Wetland complex during the study period. Previous studies have documented apparent impacts from ditching and drainage activities in the 1970s on Zoige wetland hydrology [17,19,26], while this effect may be overestimated as suggested by a recent field investigation in 2012. A recent field survey found that most of these ditches were nearly filled with silt deposits up to the ground surface, indicating a general decline in drainage impacts from these ditches since they were first constructed in the 1970s [48]. Moreover, as the WR and BR basins were both dug by similar ditch densities, *i.e.*, 0.060 km· km^{-2} and 0.066 km· km^{-2}, respectively [28,49],

the similar ditching densities minimize potential impacts on differences between the WR and BR basins and cannot fully explain the observed hydrological differences between the two basins from 1985 to 2007. In addition, ditches can promote wetland drainage and thus result in more discharge if other hydrological conditions remain the same [50,51], but the *in-situ* hydrological records showed the contrary results in the two Zoige basins, *i.e.*, decreasing trends in discharge.

Our results also indicate that land use and cover change is not likely the major factor in explaining regional hydrological trends and differences among the uYR, BR and WR basins due to the very low proportion of the study area experiencing land use and cover changes (<0.15%; mostly occurring in the uYR basin). The satellte-based land use and cover dataset (*i.e.*, LUCC-China) indicated similar vegetation cover except for large differences in wetland areas among the three studied basins in 1985 (Figure 2 and Table 4). Though overgrazing and climate warming may be important drivers of alpine grassland degradation in the Tibetan Plateau [52], the LUCC-China dataset indicated only limited land use and cover change over the study period (*i.e.*, less than 0.15% of the total basin area), mainly occurring in the upper Yellow River basin [23]. This result was partly supported by our GIMMS3g-based analysis, which did not show significant changes in the growing-season average NDVI ($p > 0.80$) in the study area (Figure 6). Therefore, land use and land cover change is not likely the major factor controlling hydrological variation in the BR and WR basins during the study period.

4.3. Implication of Climate Warming in Alpine Wetlands

Our results demonstrate strong hydrological sensitivity of alpine wetlands to climate warming, while indicating that alpine wetlands in the TP may be subject to potential degradation under projected rapid regional warming without an accompanying increase in precipitation [3]. The vulnerability of wetlands to climate warming is generally determined by the extent to which a temperature rise would change the wetland water balance [5]. Though the satellite-based land cover and land use dataset used in this study did not show obvious changes in wetland coverage, the conversion of wetlands into other land cover types will likely occur if the terrestrial water balance of aquatic environment decreases to the point where it cannot sustain wetland function and integrity. The observed TP regional trends indicating a longer non-frozen period, enhanced ET water losses and surface drying imply increasing vulnerability of alpine wetlands to degradation under continued climate warming. Some wetlands in the TP show an apparent expansion to some extent due to warming-induced deglaciation [8]. However, stronger hydrological sensitivity of alpine wetlands to climate warming, as indicated by our findings in the Zoige wetland complex, should be taken into account when projecting the impact of future climate change on TP wetlands. This process may become even more important with the gradually weakening effects of glacial retreat on wetland expansion and formation in the TP with continued warming [18].

The hydrological response of this TP alpine wetland to recent climate warming is generally consistent with how other northern (both boreal and arctic) wetlands respond to warming, where air temperature is also a major limiting factor on surface ecological and hydrological processes [53–55]. In most northern wetlands, surface water loss through ET is mainly controlled by available energy, *i.e.*, surface albedo and net solar radiation, which is also related to the changes in surface thermal and moisture conditions [56,57]. In both alpine and northern wetlands, the existence of thick soil organic layers plays a large role in regulating hydrological sensitivity (including changes in surface ET) to climate warming due to high porosity and hydraulic conductivity of organic soil [54]. In addition, the existence of permafrost helps maintain high water tables and enhance soil saturation even under relatively dry climate conditions by limiting water infiltration to deep soil layers [58]. However, warming-induced permafrost degradation may have a much larger impact on the surface hydrology of northern wetlands underlain by greater permafrost coverage, while the potential influence of warming-induced permafrost thaw on TP wetlands is likely limited due to only sparse permafrost cover in these areas [46,59]. For example, permafrost thaw may change the hydrological connectivity

of northern wetlands, and increase surface/subsurface runoff [58,60,61], while similar impacts of permafrost thaw in TP wetlands are expected to be minimal.

5. Conclusions

In this study, we found different responses of surface runoff production of two basins with similar climate and topography but different wetland coverage in the eastern Tibetan Plateau to recent climate warming (Zoige: 0.058 °C· year^{-1}; uYR: 0.065 °C· year^{-1}, both $p < 0.05$) from 1985 to 2007. Except for the difference in wetland areas, *i.e.*, 40.1% in the BR, 17.1% in the WR and only 1.8% in the uYR, the three river basins are mainly covered by alpine meadow dominated by *Kobresia tibetica*. The basin (*i.e.*, BR) with a larger wetland proportion (40.1%) showed increasingly lower annual discharge (−0.97 m^3· s^{-1} year^{-1} or −3.5%· year^{-1}, $p < 0.01$), while no significant ($p > 0.10$) trend was observed in the WR and uYR basins. The declining discharge trend was attributed to greater sensitivity of hydrological responses of alpine wetland to climate warming, as there was less than 0.14% (~110 km^2) of the study area experiencing land use and cover changes as indicated by a satellite-based land cover record. The satellite-based surface F/T dataset showed an increasing trend in the annual non-frozen period, especially in the wetland-dominated region (2.64 day· year^{-1}, $p < 0.10$), due to a warming-induced significant advance in spring thaw onset and delay in autumn freezing. Correspondingly, the satellite-NDVI derived growing-season length showed strong extension during the same period (0.26 day· year^{-1}, $p < 0.10$) congruent with regional warming and associated F/T trends. A stronger observed increase (~1.00 mm year^{-1}, $p < 0.01$) in surface water losses from ET in the BR basin, indicated by the MPI ET record, may be altering surface moisture and thermal conditions, resulting in surface drying and runoff declining of the alpine wetlands. A large increasing trend (0.043 °C· year^{-1}, $p < 0.05$) in the vertical temperature gradient between surface air and ground (~0 cm) in wetland-dominated areas indicated from weather station measurements is consistent with drying wetland conditions. Our results demonstrate the strong sensitivity of hydrological responses of alpine wetlands to climate warming, which should be taken into account when projecting the hydrological responses of the Tibetan Plateau wetlands to future climate change.

Acknowledgments: We thank Youngwook Kim for providing the satellite-based freeze/thaw dataset. We thank the Data Center for Resources and Environmental Sciences, Chinese Academy of Sciences for providing the satellite-based Land-use and Land-cover Dataset of China and the Max Planck Institute for Biogeochemistry for providing the global evapotranspiration dataset. This work was supported by the Natural Science Fund of China (41471084 and 40901022).

Author Contributions: Wenjiang Zhang, Yonghong Yi and Kechao Song designed this study, and Wenjiang Zhang wrote this manuscript including the figures and tables. John S. Kimball and Qifeng Lu contributed significantly to the discussion of results.

Conflicts of Interest: The founding sponsors had no role in the design of the study; in the collection, analyses, or interpretation of data; in the writing of the manuscript, and in the decision to publish the results.

References

1. Aber, J.S.; Pavri, F.; Aber, S.W. High-latitude and high-altitude wetland case studies. In *Wetland Environments: A Global Perspective*; John Wiley & Sons, Ltd.: Chichester, UK, 2012; pp. 336–357.
2. Shen, M.; Zhang, G.; Cong, N.; Wang, S.; Kong, W.; Piao, S. Increasing altitudinal gradient of spring vegetation phenology during the last decade on the Qinghai–Tibetan Plateau. *Agric. For. Meteorol.* **2014**, *189–190*, 71–80. [CrossRef]
3. Yang, K.; Wu, H.; Qin, J.; Lin, C.; Tang, W.; Chen, Y. Recent climate changes over the Tibetan Plateau and their impacts on energy and water cycle: A review. *Glob. Planet. Chang.* **2014**, *112*, 79–91. [CrossRef]
4. Evans, M.; Warburton, J. The Hydrology of Upland Peatlands. In *Geomorphology of Upland Peat*; Blackwell Publishing Ltd.: Oxford, UK, 2008; pp. 28–53.
5. Winter, T.C. The vulnerability of wetlands to climate change: A hydrologic landscape perspective. *JAWRA J. Am. Water Resour. Assoc.* **2000**, *36*, 305–311. [CrossRef]

6. Chen, H.; Zhu, Q.; Peng, C.; Wu, N.; Wang, Y.; Fang, X.; Gao, Y.; Zhu, D.; Yang, G.; Tian, J.; *et al.* The impacts of climate change and human activities on biogeochemical cycles on the Qinghai-Tibetan Plateau. *Glob. Chang. Biol.* **2013**, *19*, 2940–2955. [CrossRef] [PubMed]
7. Li, J.; Shi, W. Effects of alpine swamp wetland change on rainfall season runoff and flood characteristics in the headwater area of the Yangtze River. *CATENA* **2015**, *127*, 116–123. [CrossRef]
8. Niu, Z.; Zhang, H.; Wang, X.; Yao, W.; Zhou, D.; Zhao, K.; Zhao, H.; Li, N.; Huang, H.; Li, C.; *et al.* Mapping wetland changes in China between 1978 and 2008. *Chin. Sci. Bull.* **2012**, *57*, 2813–2823. [CrossRef]
9. Waddington, J.M.; Morris, P.J.; Kettridge, N.; Granath, G.; Thompson, D.K.; Moore, P.A. Hydrological feedbacks in northern peatlands. *Ecohydrology* **2014**. [CrossRef]
10. Zhang, L.; Su, F.; Yang, D.; Hao, Z.; Tong, K. Discharge regime and simulation for the upstream of major rivers over Tibetan Plateau. *J. Geophys. Res. Atmosp.* **2013**, *118*, 8500–8518. [CrossRef]
11. Xue, Z.; Zhang, Z.; Lu, X.; Zou, Y.; Lu, Y.; Jiang, M.; Tong, S.; Zhang, K. Predicted areas of potential distributions of alpine wetlands under different scenarios in the Qinghai-Tibetan Plateau, China. *Glob. Planet. Chang.* **2014**, *123*, 77–85. [CrossRef]
12. Xu, Z.X.; Zhao, F.F.; Li, J.Y. Response of streamflow to climate change in the headwater catchment of the Yellow River basin. *Quat. Int.* **2009**, *208*, 62–75. [CrossRef]
13. Yao, T.; Masson-Delmotte, V.; Gao, J.; Yu, W.; Yang, X.; Risi, C.; Sturm, C.; Werner, M.; Zhao, H.; He, Y.; *et al.* A review of climatic controls on δ18O in precipitation over the Tibetan Plateau: Observations and simulations. *Rev. Geophys.* **2013**, *51*, 2012RG000427. [CrossRef]
14. Zhang, W.; Yi, Y.; Kimball, J.; Kim, Y.; Song, K. Climatic Controls on Spring Onset of the Tibetan Plateau Grasslands from 1982 to 2008. *Remote Sens.* **2015**, *7*, 16607–16622. [CrossRef]
15. Li, X.; Jin, R.; Pan, X.; Zhang, T.; Guo, J. Changes in the near-surface soil freeze-thaw cycle on the Qinghai-Tibetan Plateau. *Int. J. Appl. Earth Obs. Geoinform.* **2012**, *17*, 33–42. [CrossRef]
16. Zhao, L.; Ping, C.-L.; Yang, D.; Cheng, G.; Ding, Y.; Liu, S. Changes of climate and seasonally frozen ground over the past 30 years in Qinghai–Xizang (Tibetan) Plateau, China. *Glob. Planet. Chang.* **2004**, *43*, 19–31. [CrossRef]
17. Zhang, Y.; Wang, G.; Wang, Y. Changes in alpine wetland ecosystems of the Qinghai–Tibetan plateau from 1967 to 2004. *Environ. Monitor. Assess.* **2011**, *180*, 189–199. [CrossRef] [PubMed]
18. Yao, T.; Thompson, L.; Yang, W.; Yu, W.; Gao, Y.; Guo, X.; Yang, X.; Duan, K.; Zhao, H.; Xu, B.; *et al.* Different glacier status with atmospheric circulations in Tibetan Plateau and surroundings. *Nat. Clim. Chang.* **2012**, *2*, 663–667. [CrossRef]
19. Xiang, S.; Guo, R.; Wu, N.; Sun, S. Current status and future prospects of Zoige Marsh in Eastern Qinghai-Tibet Plateau. *Ecol. Eng.* **2009**, *35*, 553–562. [CrossRef]
20. Yi, S.; Xiaoyun, W.; Yu, Q.; Bo, X.; Yongjian, D. Responses of alpine grassland on Qinghai-Tibetan plateau to climate warming and permafrost degradation: A modeling perspective. *Environ. Res. Lett.* **2014**, *9*, 074014. [CrossRef]
21. Yang, K.; Qin, J.; Zhao, L.; Chen, Y.; Tang, W.; Han, M.; Lazhu; Chen, Z.; Lv, N.; Ding, B.; *et al.* A multiscale soil moisture and freeze–thaw monitoring network on the third pole. *Bull. Am. Meteorol. Soc.* **2013**, *94*, 1907–1916. [CrossRef]
22. Chen, H.; Yang, G.; Peng, C.; Zhang, Y.; Zhu, D.; Zhu, Q.; Hu, J.; Wang, M.; Zhan, W.; Zhu, E.; *et al.* The carbon stock of alpine peatlands on the Qinghai–Tibetan Plateau during the Holocene and their future fate. *Quat. Sci. Rev.* **2014**, *95*, 151–158. [CrossRef]
23. Wang, G.; Li, Y.; Wang, Y.; Chen, L. Typical alpine wetland system changes on the Qinghai-Tibet Plateau in recent 40 years. *Acta Geogr. Sin.* **2007**, *62*, 481–491.
24. Sun, G. Study on the mineral formation law, classification and reserves of the peat in the Ruoergai Plateau. *J. Nat. Resour.* **1992**, *7*, 334–346.
25. Lang, H.; Jin, S.; Niu, H. The types and evolution of the marsh plants in the Zoige region, Western Sichuan. *Acta Phytoecol. Geobot. Sin.* **1964**, *2*, 40–59.
26. Zhang, X.; Liu, H.; Baker, C.; Graham, S. Restoration approaches used for degraded peatlands in Ruoergai (Zoige), Tibetan Plateau, China, for sustainable land management. *Ecol. Eng.* **2012**, *38*, 86–92. [CrossRef]
27. Li, B.; Yu, Z.; Liang, Z.; Song, K.; Li, H.; Wang, Y.; Zhang, W.; Acharya, K. Effects of climate variations and human activities on runoff in the Zoige Alpine Wetland in the eastern edge of the Tibetan Plateau. *J. Hydrol. Eng.* **2014**, *19*, 1026–1035. [CrossRef]

28. Zhang, M.; Zha, K.; Wang, Q.; Gu, H. Qualitative evalution on blocking operations for drains of Zoige alpine wetland. *Sichuan For. Explor. Design* **2010**, *4*, 15–19. (in Chinese).
29. Chai, X.; Jin, S. The types of Zoige Alpine Marsh and its development. *Acta Geogr. Sin.* **1963**, *29*, 219–240.
30. Zhang, X. *Vegetation Map of the People's Republic of China (1:1,000,000)*; China Geological Publishing House: Beijing, China, 2007.
31. CDC. *China Daily Meteorological Data Collection (1951–2012)*; China Meteorological Data Sharing Center: Beijing, China, 2013.
32. Liu, J.; Kuang, W.; Zhang, Z.; Xu, X.; Qin, Y.; Ning, J.; Zhou, W.; Zhang, S.; Li, R.; Yan, C.; *et al.* Spatiotemporal characteristics, patterns, and causes of land-use changes in China since the late 1980s. *J. Geogr. Sci.* **2014**, *24*, 195–210. [CrossRef]
33. Buermann, W.; Parida, B.; Jung, M.; MacDonald, G.M.; Tucker, C.J.; Reichstein, M. Recent shift in Eurasian boreal forest greening response may be associated with warmer and drier summers. *Geophys. Res. Lett.* **2014**, *41*, 2014GL059450. [CrossRef]
34. Kim, Y.; Kimball, J.S.; McDonald, K.C.; Glassy, J. Developing a global data record of daily landscape freeze/thaw status using satellite passive microwave remote sensing. *Geosci. Remote Sens. IEEE Trans.* **2011**, *49*, 949–960. [CrossRef]
35. Kim, Y.; Kimball, J.S.; Zhang, K.; McDonald, K.C. Satellite detection of increasing Northern Hemisphere non-frozen seasons from 1979 to 2008: Implications for regional vegetation growth. *Remote Sens. Environ.* **2012**, *121*, 472–487. [CrossRef]
36. Wang, S.; Wang, C.; Duan, J.; Zhu, X.; Xu, G.; Luo, C.; Zhang, Z.; Meng, F.; Li, Y.; Du, M. Timing and duration of phenological sequences of alpine plants along an elevation gradient on the Tibetan Plateau. *Agric. For. Meteorol.* **2014**, *189–190*, 220–228. [CrossRef]
37. Pinzon, J.; Tucker, C. A non-stationary 1981–2012 AVHRR NDVI3g time series. *Remote Sens.* **2014**, *6*, 6929–6960. [CrossRef]
38. Jönsson, A.M.; Eklundh, L.; Hellström, M.; Bärring, L.; Jönsson, P. Annual changes in MODIS vegetation indices of Swedish coniferous forests in relation to snow dynamics and tree phenology. *Remote Sens. Environ.* **2010**, *114*, 2719–2730. [CrossRef]
39. Jung, M.; Reichstein, M.; Margolis, H.A.; Cescatti, A.; Richardson, A.D.; Arain, M.A.; Arneth, A.; Bernhofer, C.; Bonal, D.; Chen, J.; *et al.* Global patterns of land-atmosphere fluxes of carbon dioxide, latent heat, and sensible heat derived from eddy covariance, satellite, and meteorological observations. *J. Geophys. Res. Biogeosci.* **2011**, *116*, G00J07. [CrossRef]
40. Baldocchi, D.; Falge, E.; Gu, L.; Olson, R.; Hollinger, D.; Running, S.N.; Anthoni, P.; Bernhofer, C.; Davis, K.; Evans, R.; *et al.* FLUXNET: A new tool to study the temporal and spatial variability of ecosystem-scale carbon dioxide, water vapor, and energy flux densities. *Am. Meteorol. Soc. Bull.* **2001**, *82*, 2415–2434. [CrossRef]
41. Fan, X. *Influence of Vegetation Coverage on Evapotranspiration Procees of Alpine Meadows in the Source Region of Yangtze River*; Lanzhou University: Lanzhou, China, 2011.
42. Qin, J.; Yang, K.; Liang, S.; Guo, X. The altitudinal dependence of recent rapid warming over the Tibetan Plateau. *Clim. Chang.* **2009**, *97*, 321–327. [CrossRef]
43. Lu, C.; Wang, L.; Xie, G.; Leng, Y. Altitude Effect of Precipitation and Spatial Distribution of Qinghai-Tibetan Plateau. *J. Mt. Sci.* **2007**, *25*, 655–663.
44. Wu, G.-L.; Ren, G.-H.; Wang, D.; Shi, Z.-H.; Warrington, D. Above- and below-ground response to soil water change in an alpine wetland ecosystem on the Qinghai-Tibetan Plateau, China. *J. Hydrol.* **2013**, *476*, 120–127. [CrossRef]
45. Su, Z.; Wen, J.; Dente, L.; van der Velde, R.; Wang, L.; Ma, Y.; Yang, K.; Hu, Z. The Tibetan Plateau observatory of plateau scale soil moisture and soil temperature (Tibet-Obs) for quantifying uncertainties in coarse resolution satellite and model products. *Hydrol. Earth Syst. Sci.* **2011**, *15*, 2303–2316. [CrossRef]
46. Wang, G.; Bai, W.; Li, N.; Hu, H. Climate changes and its impact on tundra ecosystem in Qinghai-Tibet Plateau, China. *Clim. Chang.* **2011**, *106*, 463–482. [CrossRef]
47. Kovářová, M.; Pokorný, J. Comparison of long-term monitoring of temperature and precipitation between wetland and other ecosystems. *Ecohydrology* **2010**, *3*, 445–456. [CrossRef]
48. Zhang, W.; Lu, Q.; Song, K.; Qin, G.; Wang, Y.; Wang, X.; Li, H.; Li, J.; Liu, G.; Li, H. Remotely sensing the ecological influences of ditches in Zoige Peatland, eastern Tibetan Plateau. *Int. J. Remote Sens.* **2014**, *35*, 5186–5197. [CrossRef]

49. Yang, F. Assessing the mire marsh of Zoige Plateau. *Chin. J. Resour. Explor. Prot.* **1988**, *4*, 24–30.
50. Holden, J.; Evans, M.G.; Burt, T.P.; Horton, M. Impact of land drainage on peatland hydrology. *J. Environ. Qual.* **2006**, *35*, 1764–1778. [CrossRef] [PubMed]
51. Strack, M.; Waddington, J.M.; Bourbonniere, R.A.; Buckton, E.L.; Shaw, K.; Whittington, P.; Price, J.S. Effect of water table drawdown on peatland dissolved organic carbon export and dynamics. *Hydrol. Process.* **2008**, *22*, 3373–3385. [CrossRef]
52. Zhang, Y.; Gao, Q.; Dong, S.; Liu, S.; Wang, X.; Su, X.; Li, Y.; Tang, L.; Wu, X.; Zhao, H. Effects of grazing and climate warming on plant diversity, productivity and living state in the alpine rangelands and cultivated grasslands of the Qinghai-Tibetan Plateau. *Rangel. J.* **2015**, *37*, 57–65. [CrossRef]
53. Moore, P.A.; Pypker, T.G.; Waddington, J.M. Effect of long-term water table manipulation on peatland evapotranspiration. *Agric. For. Meteorol.* **2013**, *178–179*, 106–119. [CrossRef]
54. Petrone, R.M.; Rouse, W.R.; Marsh, P. Comparative surface energy budgets in western and central subarctic regions of Canada. *Int. J. Climatol.* **2000**, *20*, 1131–1148. [CrossRef]
55. Runkle, B.R.K.; Wille, C.; Gažovič, M.; Wilmking, M.; Kutzbach, L. The surface energy balance and its drivers in a boreal peatland fen of northwestern Russia. *J. Hydrol.* **2014**, *511*, 359–373. [CrossRef]
56. Sonnentag, O.; Van Der Kamp, G.; Barr, A.G.; Chen, J.M. On the relationship between water table depth and water vapor and carbon dioxide fluxes in a minerotrophic fen. *Glob. Chang. Biol.* **2010**, *16*, 1762–1776. [CrossRef]
57. Wu, J.; Kutzbach, L.; Jager, D.; Wille, C.; Wilmking, M. Evapotranspiration dynamics in a boreal peatland and its impact on the water and energy balance. *J. Geophys. Res. Biogeosci.* **2010**, *115*, G04038. [CrossRef]
58. Connon, R.F.; Quinton, W.L.; Craig, J.R.; Hayashi, M. Changing hydrologic connectivity due to permafrost thaw in the lower Liard River valley, NWT, Canada. *Hydrol. Process.* **2014**, *28*, 4163–4178. [CrossRef]
59. Eugster, W.; Rouse, W.R.; Pielke Sr, R.A.; McFadden, J.P.; Baldocchi, D.D.; Kittel, T.G.F.; Chapin, F.S.; Liston, G.E.; Vidale, P.L.; Vaganov, E.; *et al.* Land-atmosphere energy exchange in Arctic tundra and boreal forest: Available data and feedbacks to climate. *Glob. Chang. Biol.* **2000**, *6*, 84–115. [CrossRef]
60. Grippa, M.; Mognard, N.M.; Le Toan, T.; Biancamaria, S. Observations of changes in surface water over the western Siberia lowland. *Geophys. Res. Lett.* **2007**, *34*, L15403. [CrossRef]
61. Woo, M.-K.; Guan, X.J. Hydrological connectivity and seasonal storage change of tundra ponds in a polar oasis environment, Canadian High Arctic. *Permaf. Periglac. Process.* **2006**, *17*, 309–323. [CrossRef]